SPACE-TIME SPREADING ASSISTED ADAPTIVE QAM AIDED MULTICARRIER DS-CDMA VIDEO TELEPHONY

J.Y. Chung, H. Wei and L. Hanzo[1]

School of ECS, University of Southampton, SO17 1BJ, UK.
Tel: +44-23-8059-3125, Fax: +44-23-8059-4508
Email:lh[1]@ecs.soton.ac.uk, http://www-mobile.ecs.soton.ac.uk

ABSTRACT

A Space-Time Spreading (STS) assisted near-instantaneously Adaptive Quadrature Amplitude Modulated (AQAM) Multicarrier CDMA (MC-DSCDMA) video transceiver is proposed and investigated. When the STS scheme is invoked for spreading the signal of each sub-carrier to multiple transmit antennas, the effects of channel-induced fading are substantially mitigated. Furthermore, turbo convolutional coding is invoked for enhancing the achievable BER versus SNR performance. The AQAM-aided STS MC-CDMA system was capable of maintaining a near-constant target BER and hence a near-constant video PSNR across a wide range of channel qualities, requiring a Signal-to-Noise Ration (SNR) as low as 7dB for achieving an perceptually pleasing video quality.

1. INTRODUCTION

Space-Time Spreading (STS) [1] constitutes a relative of space-time coding [2], specifically designed for CDMA systems, where the specific spreading codes of [1] are used for mapping the information bits to be transmitted to multiple transmit antennas. The operation of the STS scheme used was illustrated in graphical terms in Figures 8.7 to 8.9 of [3, pp. 303-305], which constitutes a powerful fast-fading counter-measure. Multicarrier Directy-Sequence CDMA (MC-DSCDMA) [3] constitutes the most flexible known transceiver scheme, since it has a high number of parameters, which can be conveniently configured for operation in arbitrary propagation environments. Hence MC-DSCDMA is considered to be the most likely air-interface candidate for the next generation wireless systems. The combination of STS and MC-CDMA becomes fairly resilient against the effects of fast fading, while the slow fading is conveniently combatted by the employment of near-instantaneously Adaptive Quadrature Amplitude Modulated (AQAM) [4], which was also adopted for employment of the High Speed Data Packet Access (HSDPA) mode of the third-generation wireless systems [5]. Finally, turbo convolutional coding [2] was invoked for enhancing the achievable BER versus SNR performance of the system.

2. SYSTEM OUTLINE

Let us now consider the architecture of the STS [3] assisted MC DS-CDMA scheme [6, 3] using U number of subcarriers and T_x transmitter antennas, but only a single receiver antenna. A synchronous MC DS-CDMA scheme designed for the downlink is considered, where the K users' signals are transmitted synchronously.

The financial support of the Mobile VCE, UK is gratefully acknowledged.

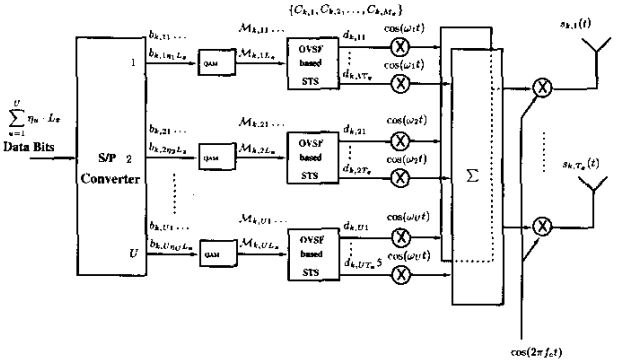

Figure 1: Schematic of the OVSF STS-aided MC-CDMA transmitter

The transmitter schematic of the kth user is shown in Figure 1, where the transmission of complex data symbols using QAM modulation and real-valued spreading [1, 3] was considered. As shown in Figure 1, at the transmitter a block of $\sum_{u=1}^{U} \eta_u \cdot L_x$ number of data bits having a bit duration of T_b is Serial-Parallel (S-P) converted to U parallel sub-blocks, where η_u is the number of Bits Per Symbol (BPS) transmitted by the QAM scheme on the uth subcarrier and L_x is the number of QAM symbols per space-time spreading sub-block. For example, if BPSK and 64QAM are invoked on the uth subcarrier, the corresponding value of η_u will be 1 and 6, respectively. Hence, each space-time spreading sub-block has $\eta_u L_x$ data bits, generating L_x modulated symbols given by $\{\mathcal{M}_{k,u1}, \ldots \mathcal{M}_{k,uL_x}\}$. These modulated symbols are space-time spread using the schemes of [1, 3] with the aid of M_x number of OVSF STS spreading codes, for example by the codes $\{c_{k,1}(t), c_{k,2}(t), \ldots, c_{k,M_x}(t)\}$, $k = 1, 2, \ldots, K$ and mapped to T_x number of transmitter antennas. Since the bits to be transmitted are mapped to the multi-bit QAM symbols as well as to T_x number of transmit antennas, the symbol duration of the STS signals is expanded to UL_xT_b, and the number of chips of the OVSF codes becomes $UL_xT_b/T_c = UL_xN$, where we have $N = T_b/T_c$, while T_c represents the chip-duration of the orthogonal spreading codes. The OVSF STS codes assume the form of

$$c_{k,i}(t) = \sum_{j=0}^{UL_xN-1} c_{k,i}[j] P_{T_c}(t - jT_c), \qquad (1)$$

where we have $c_{k,i}[j] \in \{+1, -1\}$. The OVSF STS codes obey the relationship of $\sum_{l=0}^{UL_xN} c_{i,m}[l]c_{j,n}[l] = 0$, whenever we have $i \neq j$ or $m \neq n$. Furthermore, $P_{T_c}(t)$ represents the chip waveform defined over the interval of $[0, T_c)$. Since the maximum available number of the OVSF codes having UL_xN chips is UL_xN and each user requires M_x number of OVSF codes, the maximum number of users supported by these orthogonal codes is $K_{max} = UL_xN/M_x$. As seen in Fig.1, following STS, each STS block generates T_x number of parallel signals to be mapped to the T_x number of transmitter antennas. Finally, the Inverse Fast Fourier Transform (IFFT) is invoked for carrying out multicarrier modulation [3, 7], and the IFFT block's output signal is transmitted using one of the transmitter antennas.

The operation of the STS scheme is described below. For example, for the case of $L_x = M_x = T_x = 2$, the MC DS-CDMA signals transmitted by antenna 1 and 2 can be simply expressed as [3]:

$$\mathbf{s}_k(t) = \begin{pmatrix} s_{k1}(t) \\ s_{k2}(t) \end{pmatrix} = \sqrt{\frac{2E_b}{4UT_b}} \begin{pmatrix} \sum_{u=1}^{U}[c_{k,1}\mathcal{M}_{k,u1} + c_{k,2}\mathcal{M}_{k,u2}] \times \cos[2\pi(f_c + f_u)t] \\ \sum_{u=1}^{U}[c_{k,1}\mathcal{M}_{k,u2} - c_{k,2}\mathcal{M}_{k,u1}] \times \cos[2\pi(f_c + f_u)t] \end{pmatrix} \quad (2)$$

By contrast, for the case of $L_x = M_x = T_x = 4$, the MC DS-CDMA signals transmitted by antenna 1, 2, 3 and 4, respectively, may be formulated as [3]:

$$\mathbf{s}_k(t) = \begin{pmatrix} s_{k1}(t) \\ s_{k2}(t) \\ s_{k3}(t) \\ s_{k4}(t) \end{pmatrix} = \sqrt{\frac{2E_b}{16UT_b}} \times \begin{pmatrix} \sum_{u=1}^{U}[c_{k,1}\mathcal{M}_{k,u1} + c_{k,2}\mathcal{M}_{k,u2} + c_{k,3}\mathcal{M}_{k,u3} + c_{k,4}\mathcal{M}_{k,u4}]\cos[2\pi(f_c + f_u)t] \\ \sum_{u=1}^{U}[c_{k,1}\mathcal{M}_{k,u2} - c_{k,2}\mathcal{M}_{k,u1} - c_{k,3}\mathcal{M}_{k,u4} + c_{k,4}\mathcal{M}_{k,u3}]\cos[2\pi(f_c + f_u)t] \\ \sum_{u=1}^{U}[c_{k,1}\mathcal{M}_{k,u3} + c_{k,2}\mathcal{M}_{k,u4} - c_{k,3}\mathcal{M}_{k,u1} - c_{k,4}\mathcal{M}_{k,u2}]\cos[2\pi(f_c + f_u)t] \\ \sum_{u=1}^{U}[c_{k,1}\mathcal{M}_{k,u4} - c_{k,2}\mathcal{M}_{k,u3} + c_{k,3}\mathcal{M}_{k,u2} - c_{k,4}\mathcal{M}_{k,u1}]\cos[2\pi(f_c + f_u)t] \end{pmatrix}. \quad (3)$$

The specific spreading action of the STS scheme was illustrated in graphical terms in Figure 8.7 to 8.9 of [3, pp. 303-305]. The STS scheme constitutes a powerful fast-fading countermeasure, which is conveniently complemented by adaptive modulation techniques that excel in mitigating the effects slow shadow fading, rather than fast-fading. Hence in the next section adaptive modulation is considered.

3. ADAPTIVE QAM AND STS ASSISTED MC DS-CDMA

3.1. Adaptive Mode-Switching and Learning for QAM

We considered a practically-motivated Adaptive QAM (AQAM) mode switching approach, which is based on the philosophy of *learning* the switching thresholds [8] in an on-line fashion so that the system becomes capable of maximising the achievable throughput expressed in terms of Bits Per Symbol (BPS). This learning schemes does not utilise the time-variant AQAM mode switching thresholds designed by Torrance and Hanzo [9] using Powell's optimisation. The learning-based scheme also refrains from using analytical by computed switching thresholds, or any other assumptions concerning the operating environment. The only necessary side information required by this scheme [8] is the current estimated BER $p_e(\gamma)$ (or the Frame Error Rate (FER)) and the target BER P_{th} of the system. The basic philosophy is that when the current BER $p_e(\gamma)$ is lower than the target BER P_{th}, this indicates that the system is capable of improving the achievable BPS throughput and hence it will reduce the switching thresholds for the sake of maximizing the throughput. By the contrast, when the current BER $p_e(\gamma)$ is higher than the target BER P_{th}, then the system may be overwhelmed by transmission errors and hence the algorithm will increase the switching thresholds for the sake of reducing the system's throughput.

In our investigations we considered a five-mode AQAM scheme, associated with the AQAM mode switching threshold set of $s = \{s_1, s_2, s_3, s_4\}$ designed for BPSK, QPSK, 16QAM, 64QAM, respectively. For the sake of simplicity, we assumed that the AQAM threshold difference $(s_2 - s_1), (s_3 - s_1), (s_4 - s_1)$ between the different modulation schemes was the same as in Torrance's scheme [], and we denoted them by $\triangle_{21}, \triangle_{31}, \triangle_{41}$, respectively. In other words, once we obtained the switching threshold s_1, we knew all the switching thresholds. Similarly, once we adjusted the switching threshold s_1, all the other switching thresholds were considered to be adjusted. Controlling the threshold s_1 is based on the current BER performance $p_e(\gamma)$, where the switching thresholds can be adaptively updated as follows [8]:

$$\begin{aligned} s_1(t) &= s_1(t-1) + \mu \cdot \text{sign}[p_e(\gamma) - P_{th}], \\ s_2(t) &= s_1(t) + \triangle_{21}, \\ s_3(t) &= s_1(t) + \triangle_{31}, \\ s_4(t) &= s_1(t) + \triangle_{41}, \end{aligned} \quad (4)$$

where $0 < \mu < 1$ is the threshold control step-size. Perfect estimation of the current BER was assumed, although in practice the accurate estimation of the short-term 'in-burst-BER' of a transmission burst is a challenging task [4].

4. SYSTEM PARAMETERS AND CHANNEL MODELS

The simulation parameters used in our STS MC-DS CDMA system are listed in Table 1. Channel coding techniques are capable of substantially improving achievable performance of the communication systems, in particular the family of turbo codes. The basic configurations of the turbo codes used in conjunction with the various modems are summarised in Table 1. In our system, a burst-by-burst adaptive transmission scheme was employed, each transmission burst having a fixed number of symbols, namely $L = 240$. A half-rate turbo code having a memory of $v = 3$ was used in our proposed system. The QCIF MPEG-4 video [10] coded bitrate was 69kbps at a frame scanning rate of 30 frames/sec., while the turbo-coded bitrate was 150 kbits/s. A two-path equal-weight

Parameter	Value
Channel type	Uncorrelated non-disperssive Rayleigh fading for each subcarrier
Spreading factor (OVSF)	32
No. of MC-CDMA subcarriers	16
Receiver type	RAKE/MF
Diversity	Space Time Spreading
No. of STS antennas	$T_x = 1, 2, 4$ and 8
Transmission burst length	120 bits
No. of users	32
Modulation type	BPSK, 4QAM, 16QAM, 64QAM
Channel code	1/2-rate turbo code
Channel coded bitrate	150kbps
Interleaver length	960 bit
No. of turbo decoder iterations	4
Video codec	MPEG-4
Video frame-rate	30 frame/sec
Video format	176 x 144 QCIF
Video bitrate	69kbps

Table 1: System parameters

symbol-spaced CIR was used. Again, all system parameters are summarised in Table 1.

5. PERFORMANCE RESULTS

Our experiments commence by investigating a fixed-mode scheme invoking a QPSK modem. In Figure 2, the BER performance of the half-rate turbo coded fix-mode QPSK system is presented using the various STS MC-CDMA transmitter schemes using $T_x = 1, 2, 4$ and 8 antennas for supporting 32 users. As expected, the scheme employing $T_x = 8$ transmitter antennas exhibits the highest BER performance, followed by the scheme having $T_x = 4$ transmitter antennas, etc.

For the sake of comparison, in the context of various video sequences having different motion activities, our simulations were carried out using the (174 x 144)-pixel Quarter Common Intermediate Format (QCIF) "Miss America", "Foreman" and "News" video sequences encoded at a near-constant video bitrate of 69 kbps. The corresponding video PSNR versus channel SNR performance is shown in Figure 3. Obverse that for the QPSK modulation scheme and a 1/2 coding rate, the $Tx = 1$ scheme is capable of achieving a perfect channel PSNR video performance at the channel SNR (CSNR) of approximately 12 dB, while the $Tx = 2$ scheme required a CSNR of 9 dB. Furthermore, the $Tx = 4$ scheme required a CSNR of 6 dB and finally the $Tx = 8$ scheme necessitated a CSNR of 5 dB.

Let us now characterise the achievable performance of the MC DS-CDMA system considered in conjunction with AQAM. The AQAM-aided STS MC-CDMA system was configured for maintaining a near-constant BER. More explicitly, in our experiments the adaptive thresholds were adjusted for maintaining the target BER of $10^{-3}, 10^{-4}$and 10^{-5}. The MPEG-4 video PSNR versus CSNR performance of the proposed transceiver is portrayed in Figures 4 to 6 when configuring the AQAM modem to operate at target BERs of $10^{-3}, 10^{-4}$ and 10^{-5}, respectively. This alloawed us to maintain a near-constant video quality, regardless of the channel SNR. Observe for example that as shown in Figure 4, at the

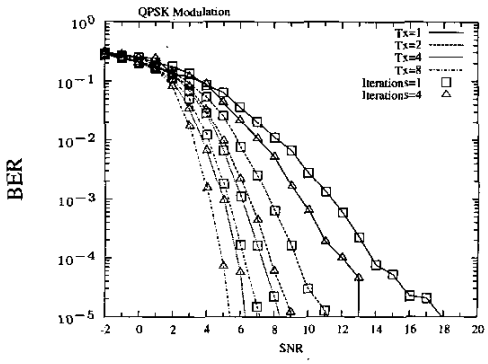

Figure 2: BER performance of STS assisted MC DS-CDMA when a QPSK scheme and half-rate turbo coding were employed. The number of antennas was $T_x = 1, 2, 4, 8$ and the number of turbo decoding iterations was I =1 and 4, respectively.

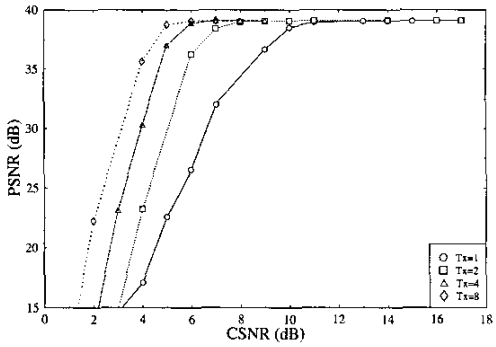

Figure 3: MPEG-4 video PSNR performance of STS assisted MC DS-CDMA when a QPSK scheme and half-rate turbo coding using four iterations were employed. The number of antennas was $T_x = 1, 2, 4, 8$.

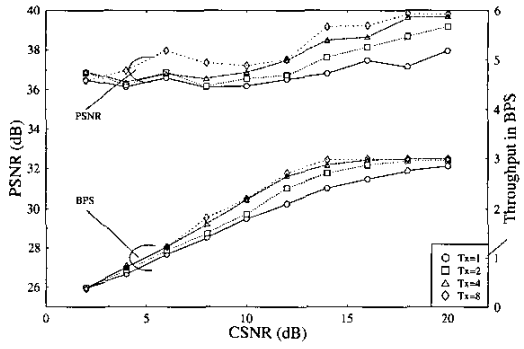

Figure 4: MPEG-4 video PSNR versus channel SNR performance of AQAM aided MC DS-CDMA. The switching thresholds were configured for maintaining a target **BER of 10^{-3}**.

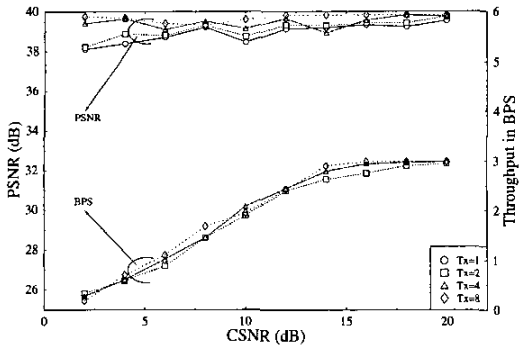

Figure 5: MPEG-4 video PSNR versus channel SNR performance of AQAM aided MC DS-CDMA. The switching thresholds were configured for maintaining a target **BER of 10^{-4}**.

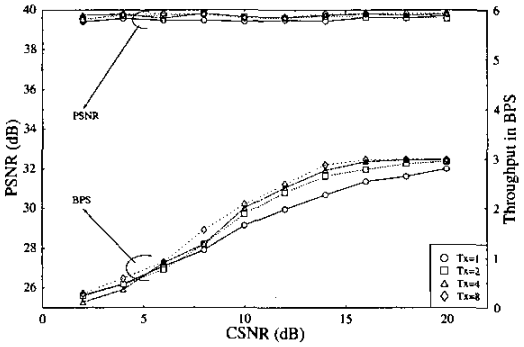

Figure 6: MPEG-4 video PSNR versus channel SNR performance of AQAM aided MC DS-CDMA. The switching thresholds were configured for maintaining a target **BER of 10^{-5}**.

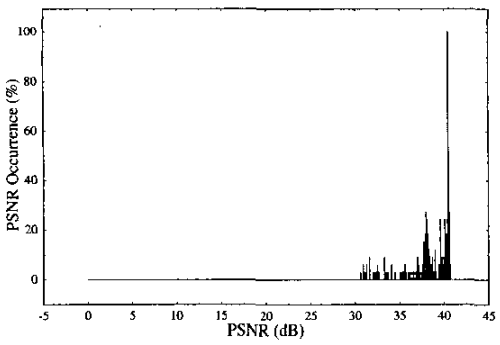

Figure 7: PDF of the MPEG-4 video PSNR of AQAM aided MC DS-CDMA. The switching thresholds were configured for maintaining a target **BER of 10^{-3}**. The number of antennas was $T_x = 8$ at CSNR = 2dB.

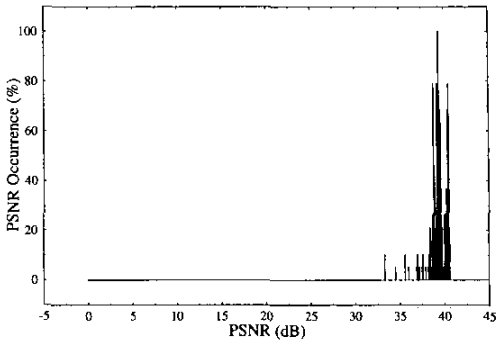

Figure 8: PDF of the MPEG-4 video PSNR of AQAM aided MC DS-CDMA. The switching thresholds were configured for maintaining a target **BER of 10^{-4}**. The number of antennas was $T_x = 8$ at CSNR = 2dB.

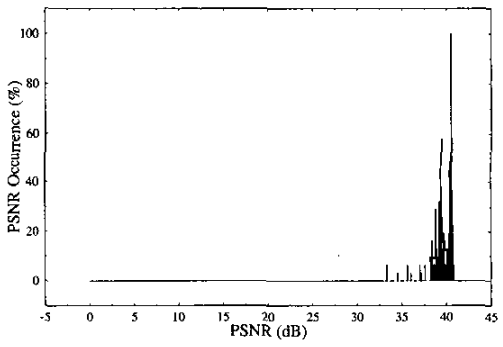

Figure 9: PDF of the MPEG-4 video PSNR of AQAM aided MC DS-CDMA. The switching thresholds were configured for maintaining a target **BER of 10^{-5}**. The number of antennas was $T_x = 8$ at CSNR = 2dB.

BER of 10^{-3} the lowest PSNR was 36.23 dB, while the highest PSNR was 39.82 dB. Similarly, in Figure 5 the PSNR ranges from 38.09 dB to 39.82 dB, while in Figure 6 from 39.41 dB to 39.82 dB. Furthermore, as also seen in Figure 4, there is a marked PSNR difference amongst the systems using a different number of antennas at the BER of 10^{-3}. This performance discrepancy becomes less dominant in Figures 5 and 6, where the target BER was lower, namely $BER = 10^{-4}$ and $BER = 10^{-5}$, respectively. These effects were further analysed and as an example Figures 7 to 9 show the PDF of the PSNR degradation for $Tx = 8$ at $CSNR = 2dB$ and at $BER = 10^{-3}, 10^{-4}$ as well as 10^{-5}.

The associated BPS throughput performance curves were also plotted in Figures 4 to 6. We can observe from these figures that the throughput of our AQAM system increased gradually, as the CSNR increased. As the channel quality improved, the 64QAM mode was employed more often, reducing the probability of using BPSK, and as a result, the achievable throughput increased.

In conclusion, the AQAM-aided STS MC-CDMA system was capable of maintaining a near-constant target BER and hence a near-constant video PSNR across a wide range of channel qualities. This is particularly so in conjunction with $T_x = 4$ or 8 antennas and a target BER of 10^{-4} or 10^{-5}.

5.1. Subjective Testing

In order to complement the objective video performance evaluations provided in the previous section, subjective video assessments were also conducted. The video quality was assessed using pairwise comparison tests, where the panel viewers were asked to express a preference between two video sequences namely 'A' or 'B' or 'neither'. A total of 12 viewers took part in these subjective tests.

Based on the subjective viewing tests, we found that the viewers were typically capable of unambiguously spotting the less corrupted, subjectively more pleasing video sequences having a lower BER.

Video A	Video B	A%	B%	Neither %
$10^{-3}(T_x = 8)$	$10^{-4}(T_x = 8)$	0%	100%	0%
$10^{-4}(T_x = 8)$	$10^{-5}(T_x = 8)$	0%	83.33%	16.67%
$10^{-3}(T_x = 8)$	$10^{-5}(T_x = 8)$	0%	100%	0%

Table 2: Results of the subjective viewing tests conducted using pairwise comparisons, where the viewers were given a choice of preference between two video sequence coded in different transmission scenarios, both having **BER = 10^{-3}**, **BER = 10^{-4}** and **BER = 10^{-5}**. The channel SNR was 8 dB.

6. CONCLUSIONS

In this study, we focused our attention on the performance of AQAM as well as STS-assisted MC DS-CDMA and studied its ability to support wireless video communications. The simulated performance of this system was characterised. A range of system performance results was presented based on both fixed-modulation schemes as well as AQAM schemes. The high-efficiency MPEG-4 video codec was employed for compressing the video signal. The proposed system ensured robust video communications using the AQAM-aided MC DS-CDMA system in a highly dispersive Rayleigh-fading environment across a wide range of channel SNR values, which was also confirmed by subjective testing.

7. REFERENCES

[1] B. Hochwald, T. L. Marzetta, and C. B. Papadias, "A Transmitter diversity scheme for wideband CDMA systems based on Space-time spreading," *IEEE Journal on Selected Areas in Communications*, vol. 19, pp. 48–60, January 2001.

[2] L. Hanzo, T. H. Liew, and B. L. Yeap, *Turbo Coding, Turbo Equalisation and Space-Time Coding for Transmission over Fading Channels*. John Wiley-IEEE Press, 2002.

[3] L. Hanzo, L. L. Yang, E. L. Kuan, and K. Yen, *Single- and Multi-Carrier DS-CDMA*. John Wiley and IEEE Press, 2003, 1060 pages.

[4] L. Hanzo, C. H. Wong, and M. S. Yee, *Adaptive Wireless Transceiver*. John Wiley.

[5] J. Blogh and L. Hanzo, *3G Systems and Intelligent Networking*. John Wiley and IEEE Press, 2002. (For detailed contents, please refer to http://www-mobile.ecs.soton.ac.uk.).

[6] L.-L. Yang and L. Hanzo, "Space-Time Spreading Assisted Broadband MC DS-CDMA," in *Proceedings of IEEE VTC'2002, Spring*, (Birmingham, Alabama, USA), May 2002.

[7] L. Hanzo, M. Münster, B. J. Choi, and T. Keller, *OFDM and MC-CDMA*. John Wiley and IEEE Press, 2003, 970 pages.

[8] C. Tang, "An Intelligent Learning Scheme for Adaptive Modulation," *In Proceedings of the IEEE Vehicular Technology Conference*, pp. 718–719, Oct 2001.

[9] J. Torrance and L. Hanzo, "Optimisation of switching levels for adaptive modulation in a slow Rayleigh fading channel," *Electronics Letters*, vol. 32, pp. 1167–1169, 20 June 1996.

[10] ISO/IEC JTC1/SC29/WG11, "Information technology - Generic coding of audio-visual objects.," in *Part 2: Visual. Draft ISO/IEC 14496-2 (MPEG-4), version 1, ISO/IEC*, (Geneva), 1998.